SCIENTIFIC REPORTS

OPEN

Electronic Properties of Fluoride and Half–fluoride Superlattices $KZnF_3/KAgF_3$ and $SrTiO_3/KAgF_3$

Received: 22 May 2015
Accepted: 01 October 2015
Published: 30 October 2015

Xiaoping Yang & Haibin Su

We present the formation of cupratelike electronic structures in $KAgF_3$–related superlattices resulted from the confinement together with structural chemical modification by using the generalized gradient approximation augmented with maximally localized Wannier functions analysis. Strong antiferromagnetic coupling found in bulk $KAgF_3$ is held in purely–fluoride $KZnF_3/KAgF_3$. Under 4% in–plane compression strain, its Fermi surface shape breaks away from the edge of electron pocket and resembles that of La_2CuO_4. While within half–fluoride $SrTiO_3/KAgF_3$, out–of–plane electronic reconstruction results in electron doping of AgF_2 plane and antiferromagnetic state instability, and the Fermi surface shape presents considerable similarity to that in $HgBaCuO_4$. These results shed light on two dimensional antiferromagnetic precursors of a new Ag^{II} family of high–temperature superconductors.

Motivated by recent susceptibility measurements of D. Kurzydlowski *et al.*[1], which indicates that $KAgF_3$ compound exhibits strong antiferromagnetic (AFM) coupling reminiscent of that found in copper(II) oxides[2,3], we carried out investigation on electronic properties of fluoride and half–fluoride $KAgF_3$–related superlattices (SLs). For a long time, the discovery of high–temperature superconductivity in under doped cuprates[4] initiated the quest for finding related transition–metal compounds with possible superconductivity. Ag^{2+} is isoelectronic to Cu^{2+} (d^9 configuration). F^- and O^{2-} are also isoelectronic ions, closed–shell species. Moreover, both F^- and O^{2-} are weak–field ligands. Previous theoretical studies[5–7] of Grochala and Hoffmann have also suggested that properly hole– or electron–doped Ag^{II} fluorides might be good superconductors, due to similarity in structure and properties between the Ag^{II} fluorides and the cuprate superconductors.

$[CuO_2]\infty$ plane with tetragonal tetra coordination of Cu (weak apical Cu–O bonds), is an essential structural element for superconductivity in cuprates. Analogous $[AgF_2]\infty$ plane with Ag centers in a tetragonal tetra coordination is still not known experimentally. However, benefit from recent development of heterostructure interface technology, superlattices containing $Ag^{II}F_2$ square lattices can be prepared by using appropriate synthetic techniques. Superlattice is consisted of alternating layers of different transition metal compounds[8–15], even technically a single atomic layer can be inserted at interface[12]. Here, interface can be used to modulate electronic structure for manipulating physical properties and generating novel phases which are not present in the bulk constituents[16–20]. In our paper, our research focus on artificial superlattice materials design and their electronic properties, different from research on real bulk Ag^{II} fluorides materials[5–7].

We investigate electronic structures, magnetic states, model hamiltonian parameters and effective Fermi surfaces (FSs) for purely–fluoride and half–fluoride superlattices $KZnF_3/KAgF_3$ and $SrTiO_3/KAgF_3$, as illustrated in the top panels of Fig. 1, and compare these with corresponding properties of the cuprate superconductors. These fluorides exhibit cupratelike band structures and strong AFM fluctuations. The energy bands around the Fermi level are sensitive to in–plane strain, and the FS shapes present considerable similarity to those in cuprates. Model hamiltonian parameters are extracted and compared to La_2CuO_4 (LCO), $HgBa_2CuO_4$ (HBCO). Strong AFM coupling found in bulk $KAgF_3$ is held

Institute of Advanced Studies, Nanyang Technological University, 50 Nanyang Avenue, 639798 Singapore. Correspondence and requests for materials should be addressed to H.S. (email: hbsu@ntu.edu.sg)

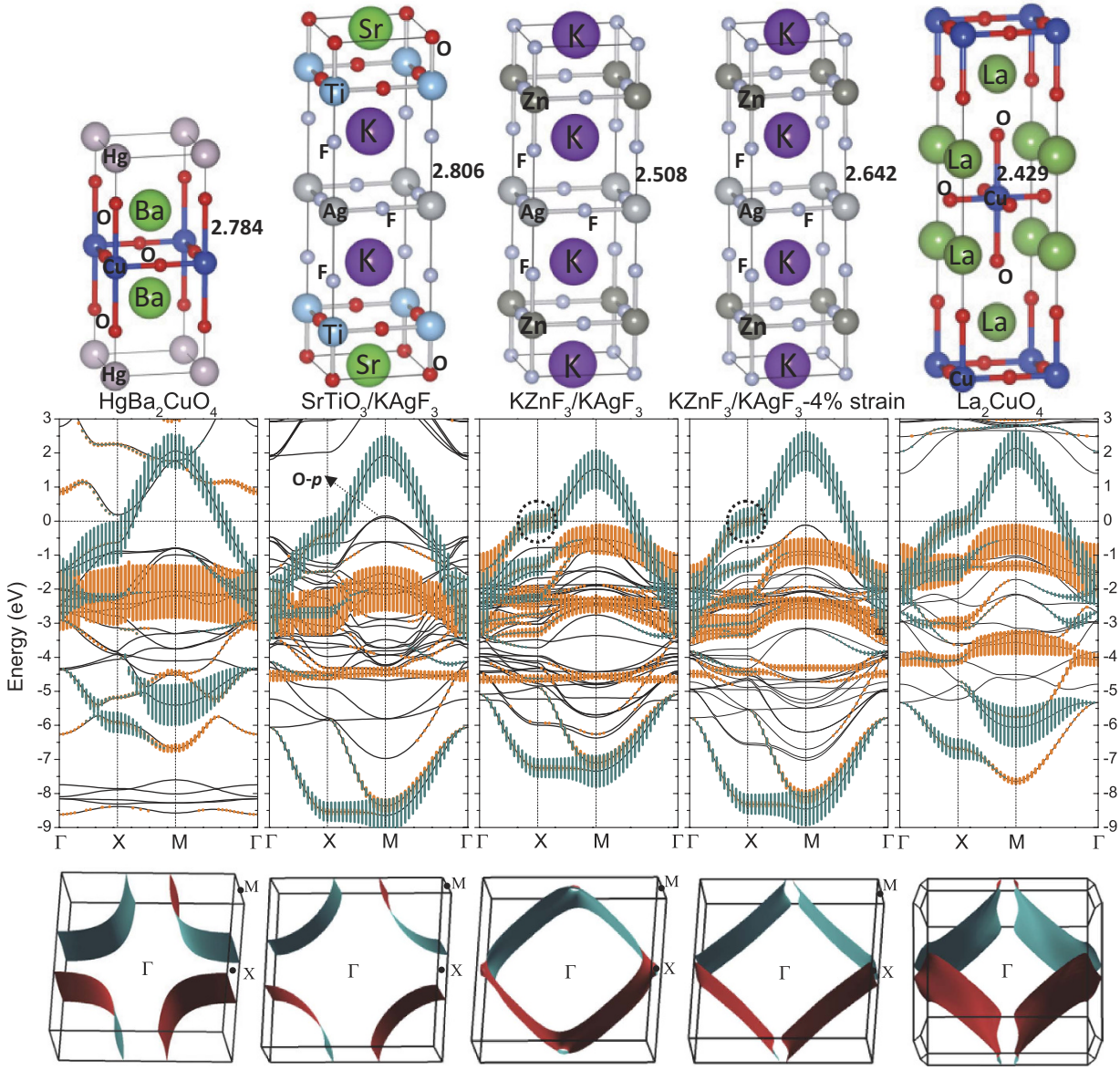

Figure 1. Schematic geometrical structures, GGA bandstructures and the effective the Fermi surfaces centered at Γ point in first Brillouin Zone from $d_{x^2-y^2}$ band for bulk HBCO, $SrTiO_3/KAgF_3$, $KZnF_3/KAgF_3$ without and with in–plane compression strain, bulk LCO from left to right. The Fermi level ε_F is set at zero. Dark cyan and orange fatbands represent contribution of $d_{x^2-y^2}$ and d_{3z^2-1} orbitals respectively.

in purely–fluoride $KZnF_3/KAgF_3$. While half–fluoride $SrTiO_3/KAgF_3$ is at the edge of superconducting transition, in which FM state becomes much high in energy, and AFM state is just below nonmagnetic (NM) state by only 11.675 meV/Ag due to out–of–plane electronic reconstruction. Our finding suggests that fluoride and half–fluoride $KAgF_3$–related SLs indeed have the potential to become 2D AFM precursors of a new Ag^{II} family of high-temperature superconductors.

Results

For the in–plane lattice constant *a*, we took that of KZnF3 (4.068 Å) for purely–fluoride $KZnF_3/KAgF_3$ SL, and took that of STO (3.905 Å) for half–fluoride $SrTiO_3/KAgF_3$ SL. The lattice constant *c* and atomic *z* coordinates were fully relaxed. The structural difference between two kinds of SLs results from different polarization strength in neighboring atomic layers of AgF_2 plane. Negatively charged F and positively charged K cation are displaced relative to each other in KF atomic layers, and thereby polarize the cation and anion planes so as to affect apical Ag–F bond length. AgF_2 layer acts as the mirror plane of whole unit cell.

A large cation–anion polarization occurs in KF plane of half–fluoride $SrTiO_3/KAgF_3$, and fluorin atoms move symmetrically against AgF_2 plane by 0.163 Å. This polarization distortion produces a local

	LCO	HBCO	$\frac{KZnF_3}{KAgF_3}$	$\frac{KZnF_3}{KAgF_3}(cp)$	$\frac{SrTiO_3}{KAgF_3}$
$d^{in-plane}_{Ag(Cu)-F(O)}$	1.894	1.941	2.034	1.953	1.953
$d^{apical}_{Ag(Cu)-F(O)}$	2.429	2.784	2.508	2.642	2.806
$E_{FM}-E_{AFM}$	177.465	127.8025	90.305	101.605	11.675*
Moment	0.542	0.495	0.442	0.447	0.268

Table 1. The in–plane and apical bond length $d^{in-plane}_{Ag(Cu)-F(O)}$ and $d^{apical}_{Ag(Cu)-F(O)}$ in Å, energy differences $E_{FM}-E_{AFM}$ in meV/Ag(Cu), and Ag/Cu atom's magnetic moment of AFM state in μ_B/Ag(Cu), for LCO, HBCO, $KZnF_3/KAgF_3$ without and with strain, $SrTiO_3/KAgF_3$. Here, *cp* between parentheses is the abbreviation for "compression". *Substituted by $E_{NM}-E_{AFM}$ since FM state becomes unavailable.

ionic dipole moment, and together with in–plane strain it leads to a large apical Ag–F distance $\left(d^{apical}_{Ag-F}=2.806\text{Å}\right)$. This apical Ag–F bond length is more close to those of cuprates than recent reported 3.405 Å for $SrTiO_3/CsAgF_3$ SL[20], due to the smaller size of the K^+ cation. However, in purely–fluoride $KZnF_3/KAgF_3$ SL, polarization distortion is weak, and is just 0.004 Å toward AgF_2 plane. As a result, apical Ag–F bond length is smaller than that in $SrTiO_3/KAgF_3$ by 0.298 Å.

An evolution of Ag-e_g states with structural chemical modification can be clearly observed in band structures of Fig. 1. Local ionic dipole moment perturbs electrostatic potential and changes band positions around the Fermi level. Spin–polarized GGA calculations give nonmagnetic ground state for both superlattices. Figure 1 shows energy bands of $SrTiO_3/KAgF_3$ and $KZnF_3/KAgF_3$ SLs in a 12 eV region around the Fermi level $\varepsilon_F\equiv 0$ and along the symmetry–lines Γ–X–M–$\Gamma=(0,0,0)-\left(\frac{\pi}{a},0,0\right)-\left(\frac{\pi}{a},\frac{\pi}{a},0\right)-(0,0,0)$. The energy bands of bulk LCO and HBCO are also plotted in Fig. 1 for comparison. For SLs, electronic properties around ε_F are still mainly controlled by Ag-e_g bands, which are above the filled O/F-2*p* and Ag-t_{2g} bands, and below the empty Ti-3*d*/Zn-4*s* bands. We plot $d_{x^2-y^2}$ (dark cyan) and d_{3z^2-1} (orange) fatbands around ε_F to disclose their orbital contribution. For $KZnF_3/KAgF_3$ SL, Ag–$d_{x^2-y^2}$ antibonding band is just below the Fermi level at X point, and resembles that of LCO. But Ag–e_g antibonding band's width is smaller than that of LCO and HBCO. Since electronic properties are subject to electron– and orbital–lattice couplings in perovskite–like materials, similar calculation is made for $KZnF_3/KAgF_3$ SL with an additional in–plane lattice constants of 3.905 Å. Energy bands are found to be sensitive to in–plane strain, and this 4% compression strain increases band width close to that of LCO. However, in $SrTiO_3/KAgF_3$ case, the antibonding band between Ag–d_{3z^2-1} and F-*p* states disappears due to the weak mixing of Ag-3*d* and F-*p* states in *z* direction. e_g bands from −3 to 2 eV appear more like that of HBCO with a larger apical Cu-O distance of 2.784 Å. Most importantly, atomic polarization results in oxygen 2*p* band edge of TiO_2 plane upshift eventually above the Fermi level and charge transfer with Ag–$d_{x^2-y^2}$ band, as occurs in $SrTiO_3/CsAgF_3$ SL[20]. The FSs centered at Γ point for LCO, HBCO and $KAgF_3$-related SLs are shown in the third row of Fig. 1. Compared to LCO (transition temperature $T_c=40$ K), the FS of HBCO ($T_c=90$ K) has the typical shape of high-T_c cuprates superconductor with constant–energy surface obviously bulging toward Γ point. The FS shape of $KZnF_3/KAgF_3$ without strain is at the edge of electron pocket and far away from that of HBCO or LCO. But the FS under 4% compression strain looks more like that of LCO. However, for $STO/KAgF_3$ with polarized electron–doping in AgF_2 plane, effective FS from Ag–$d_{x^2-y^2}$ band presents the considerable similarity to that of HBCO.

Next, we discuss the stability of magnetic states in superlattices under GGA + U_d scheme. AFM band structures indicate that $KZnF_3/KAgF_3$ SL presents a AFM insulating ground state with a energy gap of 0.445 eV. A 4% compression strain decreases energy gap to 0.232 eV. For $SrTiO_3/KAgF_3$, an AFM metallic ground state is obtained, which is aroused by charge transfer between O-p_x,p_y orbitals in TiO_2 plane and covalent hybrid orbitals of Ag–$d_{x^2-y^2}$ and F-p_x,p_y in AgF_2 plane. In Table 1, we summarize in–plane and apical bond lengths $d^{in-plane}_{Ag(Cu)-F(O)}$ and $d^{apical}_{Ag(Cu)-F(O)}$, energy difference $E_{FM}-E_{AFM}$, and magnetic moment on Ag/Cu atom in AFM state. The calculated nearest neighboring magnetic exchange coupling constant J (~$(E_{FM}-E_{AFM})$/Cu) for LCO and HBCO is in qualitative agreement with the value derived from two–magnon scattering experiments [$J_{expt}=128$ meV][21]. Generally, strong AFM coupling is held in heterostructure configuration with a confined 2D $[AgF_2]\infty$ plane. The obtained J value (~$(E_{FM}-E_{AFM})$/Ag) in undoping purely–fluoride $KZnF_3/KAgF_3$ SLs is close to that found in bulk $KAgF_3$ (~100 meV)[1], but smaller than related cuprates (see Table 1) due to less localized in 4*d*-orbitals of Ag. And in–plane compression strain increases $E_{FM}-E_{AFM}$ from 90.305 meV/Ag to 101.605 meV/Ag, similar to the trend for cuprates (*e.g.* from 127.8025 meV/Cu for HBCO to 177.465 meV/Cu for LCO in Table 1). Our finding suggests that fluoride $KAgF_3$ related SLs indeed have the potential to become precursors of a new family of high-temperature superconductors which could benefit from enhancement of the critical superconducting temperature due to strong magnetic fluctuations[22]. In half–fluoride $SrTiO_3/KAgF_3$ SL, FM state

	LCO	HBCO	$\frac{KZnF_3}{KAgF_3}$	$\frac{KZnF_3}{KAgF_3}(cp)$	$\frac{SrTiO_3}{KAgF_3}$
$d^{in-plane}_{Ag(Cu)-F(O)}$	1.894	1.941	2.034	1.953	1.953
$d^{apical}_{Ag(Cu)-F(O)}$	2.429	2.784	2.508	2.642	2.806
Δ_{e_g}	0.005	0.115	0.095	0.227	0.477
Δ_{CT}	2.305	1.476	2.624	3.247	3.459
t_{pd}	1.395	1.249	1.483	1.754	1.756
t_{pp}	0.656	0.620	0.350	0.400	0.415

Table 2. Tight–binding parameters of the six–band *p-d* model, containing the in–plane $d_{x^2-y^2}$, p_x, p_y orbitals and out–of–plane d_{3z^2-1}, p_z orbitals for LCO, HBCO, $KZnF_3/KAgF_3$ without and with in–plane strain, $SrTiO_3/KAgF_3$. Parameters include e_g crystal field splitting energies $\Delta_{\varepsilon_g} = \varepsilon_{x^2-y^2} - \varepsilon_{3z^2-1}$, charge–transfer energies $\Delta_{CT} = \varepsilon_{x^2-y^2} - \varepsilon_{p_{x(y)}}$, the two nearest–neighbor (intra–cell) hoppings t_{pd}, t_{pp} in eV. The in–plane and apical bond length $d^{in-plane}_{Ag(Cu)-F(O)}$ and $d^{apical}_{Ag(Cu)-F(O)}$ in Å are also listed to identify structural chemical difference. Here, *cp* inside parentheses is the abbreviation for "compression".

becomes much high in energy and unavailable. AFM state is just below NM state by only 11.675 meV/Ag due to out–of–plane electronic reconstruction.

Based on the aboved GGA simulations, we extract model hamiltonian parameters by MLWFs downfolding technique. Fourier transformation of the orthonormalized MLWE Hamiltonian $H(k)$, yields on–site energies and hopping integrals

$$H_{\mathbf{0}n,\mathbf{R}m} \equiv \langle \mathbf{0}n|H|\mathbf{R}m\rangle \equiv t^{\mathbf{R}}_{nm} \tag{1}$$

in a Wannier representation, where $|\mathbf{R}m\rangle$ is orthonormal MLWF Wannier function in cell $\mathbf{R}$ associated with band m, and $|\mathbf{0}n\rangle$ is MLWF Wannier function in home cell associated with band n.

We choose to downfold to a 6-band hamiltonian describing the in-plane $d_{x^2-y^2}$, p_x, p_y orbitals, and out–of–plane d_{3z^2-1}, two p_z orbitals. In particular, four parameters capture the essential physics: the e_g crystal field splitting energy $\Delta_{e_g} = \varepsilon_{x^2-y^2} - \varepsilon_{3z^2-1}$, the in–plane charge–transfer energy $\Delta_{CT} = \varepsilon_{x^2-y^2} - \varepsilon_{p_{x(y)}}$, the direct in–plane Ag–F hopping t_{pd}, and the shortest–ranged in–plane F–F hoppings t_{pp}. The extracted values are tabulated in Table 2, and corresponding interpolated band structure are shown in Fig. 2.

The hopping integrals t_{pd} and t_{pp} of LCO and HBCO are in good agreement with the 3–band model results[23,24] and the analysis of the photoelectron spectroscopy[25]. While the data of Δ_{CT} are further corrected in our model by including three additional out–of–plane orbitals. Compared to cuprates, purely–fluoride $KZnF_3/KAgF_3$ has relatively larger Δ_{e_g}, Δ_{CT}, and in–plane Ag–F hopping t_{pd}, and smaller hopping t_{pp}. In–plane compression strain increase the values of the former three parameters Δ_{e_g}, Δ_{CT} and t_{pd}, but has only a slight change on the hopping t_{pp}. Under the same in–plane lattice constant 3.905 Å, half–fluoride $SrTiO_3/KAgF_3$ has obvious larger Δ_{e_g}, Δ_{CT} and slightly increased t_{pp}, compared to purely–fluoride $KZnF_3/KAgF_3$. Across cuprate families, the charge transfer energy is an increasing linear function of Madelung potential difference for a hole between the copper and in–plane oxygen, and correlate with the maximum superconducting transition temperature $T_{c,max}$[26]. The decreasing Δ_{CT} correlates with a enhanced $T_{c,max}$. Here, half–fluoride $SrTiO_3/KAgF_3$ has a slight reduced Δ_{CT} value 3.459 eV between the silver and in–plane fluorine, compared to the reported 3.504 eV for $SrTiO_3/CsAgF_3$[20], while purely–fluoride $KZnF_3/KAgF_3$ has a obvious smaller charge transfer gap, as shown in Table 2.

Discussion

In conclusion, we investigate cupratelike electronic structures and strong AFM fluctuations effect in the proposed $KAgF_3$–related superlattices. Compared to bulk $KAgF_3$, undoping purely–fluoride $KZnF_3/KAgF_3$ SL has a similar magnetic coupling constant. A 4% in–plane compression strain stabilizes AFM state further, and makes the FS shape to deviate from the edge of electron pocket and to resemble that of LCO. In half–fluoride $SrTiO_3/KAgF_3$ SL, atomic polarization induces out–of–plane electronic reconstruction occurring between O-p_x,p_y orbitals in TiO_2 plane and covalent hybrid orbitals of Ag–$d_{x^2-y^2}$ and F-p_x,p_y in AgF_2 plane, which results in AFM state instability by a smaller energy difference $E_{NM} - E_{AFM}$ of 11.675 meV/Ag. And FS shape of half–fluoride SL presents considerable similarity to that in HBCO. Therefore, fluoride and half–fluoride $KAgF_3$–related superlattices indeed have the potential to become 2D AFM precursors of a new Ag^{II} family of high–temperature superconductors, which could benefit

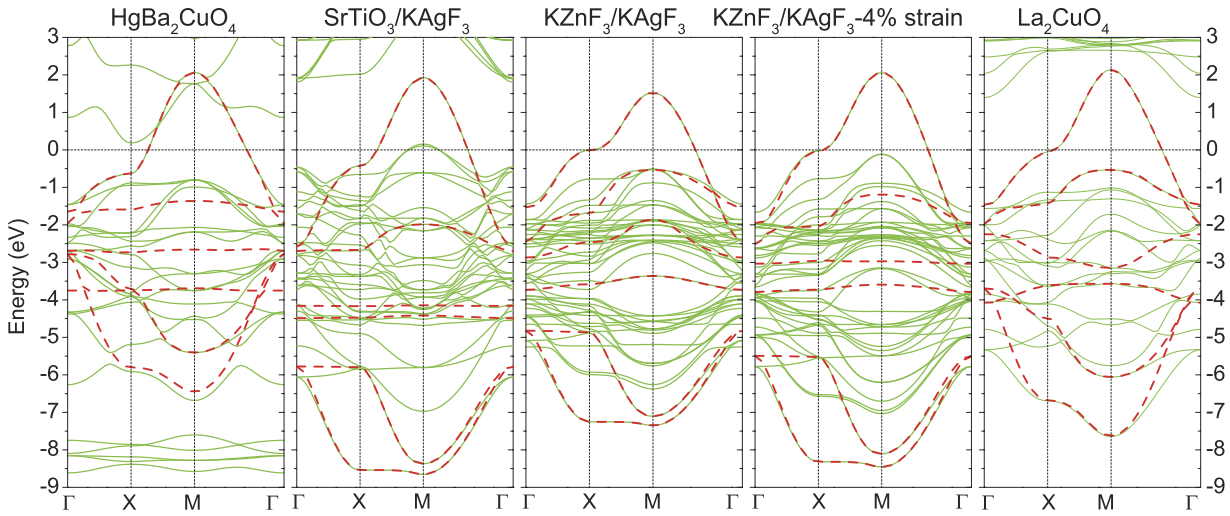

Figure 2. Effective e_g MLWF bands (red dash lines) for bulk HBCO, $SrTiO_3/KAgF_3$, $KZnF_3/KAgF_3$ without and with in-plane compression strain, bulk LCO superimposed to the GGA electronic bands (green solid lines). The Fermi level ε_F is set at zero.

from enhancement of the critical superconducting temperature due to strong magnetic fluctuation, and the relative small charge transfer gap in $KZnF_3/KAgF_3$.

Method

We carried out the numerical calculations using the Vienna *ab initio* Simulation Package (VASP)[27–30] within the framework of the generalized gradient approximation (GGA) (Perdew-Burke-Ernzerhof exchange correlation functional)[31], and recently developed maximally localized Wannier functions (MLWFs) downfolding technique[32–34]. The ion–electron interaction was modeled by the projector augmented wave (PAW) method[35,36] with a uniform energy cutoff of 500 eV. Spacing between k points was 0.02 $Å^{-1}$. The geometrcal structures of the SLs were optimized by employing the conjugate gradient technique, and in the final geometry, no force on the atoms exceeded 0.01 eV/Å. For magnetic states calculations, we used $U_d = 7.5$ eV and $J_d = 0.98$ eV for Cu-3d state[37] and a smaller $U_d = 5$ eV and $J_d = 0.98$ for Ag-4d state[38].

References

1. Kurzydlowski, D., Mazej, Z., Jaglicic, Z., Filinchuke, Y. & Grochala, W. Structural transition and unusually strong antiferromagnetic superexchange coupling in perovskite $KAgF_3$. *Chem. Commun.* **49,** 6262–6264 (2013).
2. Armitage, N. P., Fournier, P. & Greene, R. L. Progress and perspectives on electron–doped cuprates. *Rev. Mod. Phys.* **82,** 2421 (2010).
3. Tahir-Kheli, J. & Goddard, W. A. III Universal Properties of Cuprate Superconductors: Tc Phase Diagram, Room-Temperature Thermopower, Neutron Spin Resonance, and STM Incommensurability Explained in Terms of Chiral Plaquette Pairing. *J. Phys. Chem. Lett.* **1,** 1290–1295 (2010).
4. Bednorz, J. G. & Müller, K. A. Possible high T_c superconductivity in the Ba–La–Cu–O system. *Z. Phys. B* **64,** 189–193 (1986).
5. Grochala, W. & Hoffmann, R. Real and Hypothetical intermediate–valence Ag^{II}/Ag^{III} and Ag^{II}/Ag^{I} fluoride systems as potential superconductors. *Angew. Chem. Int. Ed.* **40,** 2742–2781 (2001).
6. Grochala, W., Egdell, R. G., Edwards, P. P., Mazej, Z. & Zemva, B. On the covalency of silver–fluorine bonds in compounds of silver(I), silver(II) and silver(III). *Chem Phys Chem* **4,** 997–1001 (2003).
7. Jaron, T. & Grochala, W. Prediction of giant antiferromagnetic coupling in exotic fluorides of Ag^{II}. *Phys. Stat. Sol. (RRL)* **2,** 71–73 (2008).
8. Ohtomo, A. & Hwang, H. Y. A high–mobility electron gas at the $LaAlO_3/SrTiO_3$ heterointerface. *Nature* **427,** 423–426 (2004).
9. Thiel, S., Hammerl, G., Schmehl, A., Schneider, C. W. & Mannhart, J. Tunable quasi–two–dimensional electron gases in oxide heterostructures. *Science* **313,** 1942–1945 (2006).
10. Reyren, N. *et al.* Superconducting interfaces between insulating oxides. *Science* **317,** 1196–1199 (2007).
11. Huijben, M. *et al.* Structure–property relation of $SrTiO_3/LaAlO_3$ interfaces. *Adv. Mater.* **21,** 1665–1677 (2009).
12. Jang, H. W. *et al.* Metallic and insulating oxide interfaces controlled by electronic correlations. *Science* **331,** 886–889 (2011).
13. Bozovic, I. *et al.* No mixing of superconductivity and antiferromagnetism in a high–temperature superconductor. *Nature* **422,** 873–875 (2003).
14. Logvenov, G., Gozar, A. & Bozovic, I. High–temperature superconductivity in a single copper–oxygen plane. *Science* **326,** 699–702 (2009).
15. Bollinger, A. T. *et al.* Superconductor–insulator transition in $La_{2-x}Sr_xCuO_4$ at the pair quantum resistance. *Nature* **472,** 458–460 (2011).
16. Hansmann, P. *et al.* Turning a nickelate fermi surface into a cupratelike one through heterostructuring. *Phys. Rev. Lett.* **103,** 016401 (2009).
17. Hansmann, P., Toschi, A., Yang, X. P., Andersen, O. K. & Held, K. Electronic structure of nickelates: From two-dimensional heterostructures to three-dimensional bulk materials. *Phys. Rev. B* **82,** 235123 (2010).

18. Yang, X. P. & Su, H. Polarization and electric field dependence of electronic properties in $LaAlO_3/SrTiO_3$ heterostructures. *ACS Appl. Mater. Interfaces* **3,** 3819–3823 (2011).
19. Yang, X. P. & Su, H. Electronic reconstruction and surface two-dimensional electron gas in a polarized heterostructure with a hole-doped single copper-oxygen plane. *Phys. Rev. B* **87,** 205116 (2013).
20. Yang, X. P. & Su, H. Cuprate–like Electronic Properties in Superlattices with $Ag^{II}F_2$ Square Sheet. *Scientific Reports* **4,** 5420 (2014).
21. Singh, R. R. P., Fleury, P. A., Lyons, K. B. & Sulewski, P. E. Quantitative Determination of Quantum Fluctuations in the Spin–1/2 Planar Antiferromagnet. *Phys. Rev. Lett.* **62,** 2736–2739 (1989).
22. Monthoux, P. & Pines, D. Spin–Fluctuation–Induced Superconductivity in the Copper Oxides: A Strong Coupling Calculation. *Phys. Rev. Lett.* **69,** 961–964 (1992).
23. Weber, C., Yee, C.-H., Haule, K. & Kotliar, G. Scaling of the transition temperature of hole–doped cuprate superconductors with the charge–transfer energy. *EPL* **100,** 37001 (2012).
24. Chen, X.-J. & Su, H. B. Electronic mechanism of critical temperature variation in $RBa_2Cu_3O_{7-\delta}$. *Phys. Rev. B* **71,** 094512 (2005).
25. Eskes, H., Sawatzky, G. A. & Feiner, L. F. Effective transfer for singlets formed by hole doping in the high–T_c superconductors. *Physica C* **160,** 424–430 (1989).
26. Ohta, Y., Tohyama, T. & Maekawa, S. Apex oxygen and critical temperature in copper oxide superconductors: Universal correlation with the stability of local singlets. *Phys. Rev. B* **43,** 2968–2982 (1991).
27. Kresse, G. & Hafner, J. Ab initio molecular dynamics for liquid metals. *Phys. Rev. B* **47,** 558–561 (1993).
28. Kresse, G. & Hafner, J. Ab initio molecular–dynamics simulation of the liquid–metal–amorphous–semiconductor transition in germanium. *Phys. Rev. B* **49,** 14251–14269 (1994).
29. Kresse, G. & Furthmüller, J. Efficient iterative schemes for ab initio total–energy calculations using a plane–wave basis set. *Phys. Rev. B* **54,** 11169–11186 (1996).
30. Kresse, G. & Furthmüller, J. Efficiency of ab–initio total energy calculations for metals and semiconductors using a plane–wave basis set. *Comput. Mater. Sci.* **6,** 15–50 (1996).
31. Perdew, J. P., Burke, K. & Ernzerhof, M. Generalized gradient approximation made simple. *Phys. Rev. Lett.* **77,** 3865–3868 (1996).
32. Marzari, N. & Vanderbilt, D. Maximally localized generalized Wannier functions for composite energy bands. *Phys. Rev. B* **56** 12847–12865 (1997).
33. Souza, I., Marzari, N. & Vanderbilt, D. Maximally localized Wannier functions for entangled energy bands. *Phys. Rev. B* **65** 035109 (2001).
34. Mostofi, A. A. *et al.* Wannier90: A tool for obtaining maximally–localised wannier functions. *Comput. Phys. Commun.* **178,** 685–699 (2008).
35. Kresse, G. & Joubert, D. From ultrasoft pseudopotentials to the projector augmented-wave method. *Phys. Rev. B* **59,** 1758–1775 (1999).
36. Blöchl, P. E. Projector augmented–wave method. *Phys. Rev. B* **50,** 17953–17979 (1994).
37. Anisimov, V. I., Zaanen, J. & Andersen, O. K. Band theory and Mott insulators: Hubbard U instead of Stoner I. *Phys. Rev. B* **44,** 943–954 (1991).
38. Kasinathan, D., Koepernik, K., Nitzsche, U. & Rosner, H. Ferromagnetism Induced by Orbital Order in the Charge-Transfer Insulator Cs_2AgF_4: An Electronic Structure Study. *Phys. Rev. Lett.* **99,** 247210 (2007).

Acknowledgements

We are grateful for the interesting discussions with W. Grochala and W.A. Goddard. This work was supported in part by the A*STAR SERC grant (no. 1121202012) and MOE Tier-2 grant (no. MOE2013-T2-2-049).

Author Contributions

H.B.S. conceived the project. X.P.Y. performed the calculations. All authors discussed the results, wrote and commented on the manuscript at all stages.

Additional Information

Competing financial interests: The authors declare no competing financial interests.

How to cite this article: Yang, X. and Su, H. Electronic Properties of Fluoride and Half-fluoride Superlattices $KZnF_3/KAgF_3$ and $SrTiO_3/KAgF_3$. *Sci. Rep.* **5**, 15849; doi: 10.1038/srep15849 (2015).

This work is licensed under a Creative Commons Attribution 4.0 International License. The images or other third party material in this article are included in the article's Creative Commons license, unless indicated otherwise in the credit line; if the material is not included under the Creative Commons license, users will need to obtain permission from the license holder to reproduce the material. To view a copy of this license, visit http://creativecommons.org/licenses/by/4.0/